Supporting Information

Mechanistic Study of Tumor Fluorescence Response Signal Based on a Near-Infrared Viscosity-Sensitive Probe

Tianyang Han,[a,c] Lihao Lin,[d] Huizhong Jiang,[e] Li Fan,[f] Yuewei Zhang,[a,b*]*

1. Materials and method

Materials.

Unless otherwise noted, all reagents were obtained from commercial resources and used without further purification. Tetrahydrofuran (THF), toluene (Tol), and dichloromethane (DCM) used for reactions were purified by evaporating after fully stirring with Na and using benzophenone as the indicator. All air and moisture-sensitive reactions were carried out in flame-dried glassware under a nitrogen atmosphere. The following reagents were used in the tests: Glycol (GLY), dioxane, ethanol (EtOH), toluene (Tol), methanol (MeOH), acetonitrile (MeCN), tetrahydrofuran (THF), dimethyl and sulfoxide (DMSO), all of which were purchased from Sigma-Aldrich with a purity of 95-98%. The cell colocalization stain was purchased from Beyotime Biotechnolog.

Cell lines used in this study were obtained from the Cell Bank of the Chinese Academy of Sciences (CAS), a reputable source for authenticated and quality-controlled cell lines. The cell lines were maintained and cultured according to the standard protocols provided by the cell bank.The MTT solution was prepared using MTT powder, which was purchased from Macklin.

Quantum yield test.

The QYs of the fluorophores were measured using previously reported procedures with modifications.[1] The NIR-II fluorescence emission intensities were measured under the same 808 nm excitation. The QY values of the samples were determined on the basis of five concentrations with gradient ODs at 808 nm. Using the measured ODs at 808 nm and the integrated fluorescence intensity, the quantum yield of a test sample was calculated according to the following equation:[1]

$$\varphi_x(\gamma) = \varphi_{std}(\gamma) \times \frac{F_X}{F_{std}} \times \frac{A_{std}(\gamma)}{A_x(\gamma)} \times \left(\frac{\eta_x}{\eta_{std}}\right)^2$$

Photostability.

5μM POH, ICG and IR-783 were dissolved in PBS. The fluorescence signal was monitored using a two-dimensional InGaAs camera under continuous exposure to an 808-nm laser at a power density of 65 mW/cm^2. The average fluorescence intensity of the region of interest (ROI) was plotted as a function of time.

Cell viability assessment using the 3-(4,5-Dimethylthiazol-2-yl)-2,5-diphenyltetrazolium bromide (MTT) colorimetric assay.

The 4T1, U87, C6, and L-02 cells (5k per well) were seeded into a 96-well plate (NEST) and incubated for 12 h at 37 °C in a humidified incubator with 5% CO_2. Then, DMEM solutions with 0.1, 1.0, 2.0, 5.0, and 10.0 POH were added. After 24 h of incubation, the cells were rinsed three times with PBS and 100 μL MTT (0.5 mg·mL^{-1}) solution was added. After removing the MTT solution after 4 h of incubation, 50 μL DMSO was added to each well. Placing the shaking table at a low speed for 2 h allowed the crystal to fully dissolve. The absorbance value of each well was measured at OD 570 nm using an Elisa reader (BioTek Synergy LX).

Animals and ulcerative colitis models.

All animal experiments were conducted under institutional guidelines and were approved by the Experimental Animal Ethical Committee of the First Hospital of Jilin University (Protocol number: 20210642). BALB/c mice were purchased from Liaoning Changsheng Biotechnology Co. Ltd. Bedding, nesting materials, food, and water were provided ad libitum. The ambient temperature was controlled between 20 °C to 24 °C.

Breast tumor NIR-II fluorescence imaging.

Under 808 nm excitation laser, 850 nm SP (Short Pass Filter) and 900/1000 nm LP (Long Pass Filter) were used to collect NIR-II bioimaging. POH in PBS (100 μM, 25 μL) was injected into the breast tumor (n = 3) inoculated by 4T1 cells. The NIR-II images were obtained at 0 min, 30 min, 1 h, 3 h, 6 h, 12 h, 24 h, 48 h, 72 h, and 96 h post-injection.

H&E staining.

All the tissues were fixed in 4% paraformaldehyde after harvesting. These tissues were further dehydrated, embedded in paraffin, and sectioned into 3 μm thick slides. H&E staining was then performed according to the protocol of the H&E kit (Beyotime Institute of Biotechnology, Cat. No. C0105). H&E staining images of every tissue were acquired using the Nikon Eclipse 80i microscope.

NIR-II imaging.

All mice were shaved using Nair depilatory cream and anesthetized with chloral hydrate or isoflurane before the experiment, and then placed on the imaging table. At least three mice were used as parallel controls in each imaging experiment. All NIR-I/NIR-II images were collected on a two-dimensional InGaAs array (Princeton Instruments, NIRvana-640) with a laser wavelength of 808 nm and a power density of 65 mW/cm^2.

Metabolism assessment.

Under 808 nm excitation, 900 and 1000 nm long-pass filters were used to collect NIR-II imaging under the InGaAs camera. POH in PBS (100 μM, 200 μL) were intravenously injected into six-week-old BALB/c mice (n = 3). Images were obtained at 0 min, 30 min, 1 h, 3 h, 6 h, 12 h, and 24 h post-injection.

Tumor Establishment Process.

After culturing 4T1 cells in vitro to the logarithmic growth phase, 1×10^5 cells were subcutaneously injected into the mammary fat pad of female BALB/C mice (4-6 weeks old, body weight 18-20 g). Tumor establishment was confirmed when palpable nodules appeared in the axillary region approximately five days post-injection.

Dose and Administration Time.

The probe (100 μM, 25 μL) was administered via intratumoral injection once the tumor nodules were detectable. Time intervals for imaging were specified as 0, 30 minutes, 1, 3, 6, 12, 24, 48, 72, and 96 hours post-injection.

In this study, we employed three common tumor drug delivery methods to investigate how different routes of administration affect tumor localization and therapeutic efficacy. For intravenous injection, a concentration of 100 μM was administered at a dosage of 200 μL, allowing the drug to rapidly enter systemic circulation for widespread distribution and evaluation of overall drug behavior. For round (peritumoral, subcutaneous) injection, the drug was given at the same concentration but in a volume of 25 μL to target the tissue surrounding the tumor, thereby achieving a higher local concentration and enhancing drug penetration and accumulation at the tumor margins. Similarly, for intratumoral injection, 100 μM at 25 μL was directly administered into the tumor tissue to ensure that the drug acts specifically on the tumor, further increasing the local concentration and therapeutic effect. These delivery methods, with their distinct advantages, allow for the assessment of both local and systemic drug distribution as well as precise drug localization; detailed explanations of these routes and their specific applications in our study are provided in the supplementary information.

2. Synthesis and characterizations of POH

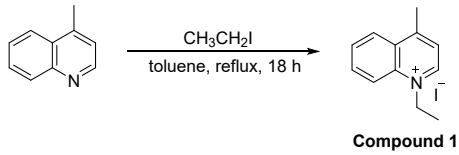

Compound 1

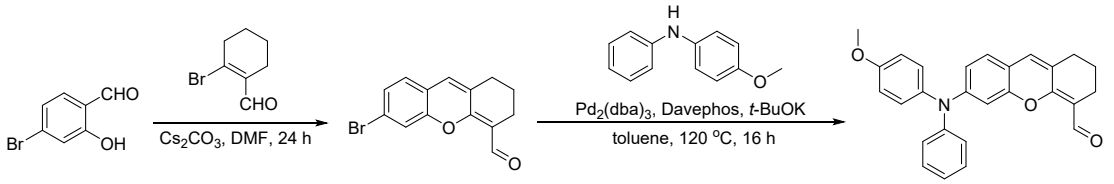

Compound 2 **Compound 3**

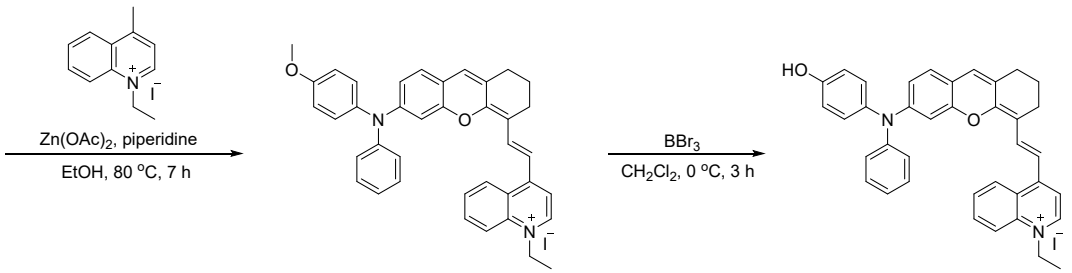

Compound 4 **POH**

Synthesis of Compound 1

4-Methylquinoline (0.858 g, 6 mmol) was dissolved in toluene (3 mL), then iodoethane (1.16 g, 7.5 mmol) was added, and the mixture was stirred at reflux for 18 h. The reaction mixture was then cooled to room temperature, and a large amount of solid was precipitated, which was washed with ethyl ether for several times and dried under vacuum to obtain **compound 1** as a green solid (1.65 g, 92% yield). ^{1}H NMR (400 MHz, DMSO-d_6) δ 9.43 (d, J = 6.0 Hz, 1H), 8.60 (d, J = 8.8 Hz, 1H), 8.55 (dd, J = 8.8, 1.2 Hz, 1H), 8.26 (ddd, J = 8.8, 6.8, 1.2 Hz, 1H), 8.10 – 8.03 (m, 2H), 5.05 (q, J = 7.2 Hz, 2H), 3.00 (s, 3H), 1.58 (t, J = 7.2 Hz, 3H). ^{13}C NMR (100 MHz, DMSO-d_6) δ 158.3, 148.1, 136.5, 135.1, 129.5, 128.9, 127.2, 122.7, 119.2, 52.5, 19.7, 15.2. HRMS (ESI-TOF): calcd. for $C_{12}H_{14}N$ $[M + H]^+$ 172.1121; found 172.1118.

Synthesis of Compound 2

To a solution of 4-bromo-2-hydroxybenzaldehyde (2 g, 10 mmol) and Cs_2CO_3 (9.75 g, 30 mmol) in dry DMF (35 mL) was added a solution of 2-bromocyclohex-1-ene-1-carbaldehyde (3.78 g, 20 mmol) in DMF (5 mL) at room temperature. The reaction mixture was stirred at 30 ^{o}C for 24 h, until starting material 4-bromo-2-hydroxybenzaldehyde was consumed. After completion of reaction, the mixture was poured into water (400 mL) and extracted with ethyl acetate (3 × 200 mL). The combined organic phase was dried over anhydrous $MgSO_4$, filtered, concentrated in vacuo, and the residue was purified by flash column chromatography eluting with (PE/EtOAc, 10:1, v/v) to afford **compound 2** as a yellow solid (1.39 g, 48% yield). ^{1}H NMR (400 MHz, $CDCl_3$) δ 10.31 (s, 1H), 7.28 (d, J = 1.2 Hz, 1H), 7.20 (dd, J = 8.0, 1.8 Hz, 1H), 7.02 (d, J = 8.4 Hz, 1H), 6.62 (s, 1H), 2.61 – 2.54 (m, 2H), 2.44 (t, J = 6.4 Hz, 2H), 1.78 – 1.68 (m, 2H). ^{13}C NMR (100 MHz, $CDCl_3$) δ 188.0, 159.6, 152.4, 130.3, 127.7, 127.1, 125.8, 123.0, 120.3, 118.8, 113.9, 30.2, 21.5, 20.3. HRMS (ESI-TOF): calcd. for $C_{14}H_{12}BrO_2$ $[M + H]^+$ 291.0015; found 291.0018.

Synthesis of Compound 3

Compound 2 (1.1 g, 3.8 mmol), 4-methoxydiphenylamine (3.78 g, 19 mmol), $Pd_2(dba)_3$ (348 mg, 0.38 mmol), DavePhos (149 mg, 0.38 mmol) and *t*-BuOK (851 mg, 7.6 mmol) were mixed in toluene (25 mL). The mixture was deaerated by flushing with argon for three times and subsequently stirred at reflux for 16 h. The mixture was then further subjected to column chromatography (PE/DCM/DMK, 20:5:1, v/v/v) to afford **Compound 3** as a brown yellow solid (0.964 g, 62% yield). ^{1}H NMR (500 MHz, $CDCl_3$) δ 10.19 (s, 1H), 7.32 – 7.27 (m, 2H), 7.15 – 7.05 (m, 5H), 6.95 (d, J = 7.5 Hz, 1H), 6.91 – 6.84 (m, 2H), 6.70 – 6.64 (m, 2H), 6.62

(s, 1H), 3.82 (s, 3H), 2.55 (t, J = 5.5, 2H), 2.42 (t, J = 6.0 Hz, 2H), 1.75 – 1.66 (m, 2H). ^{13}C NMR (100 MHz, $CDCl_3$) δ 187.6, 161.1, 157.1, 153.3, 150.3, 146.9, 139.5, 129.6, 128.1, 127.1, 126.3, 124.9, 123.9, 116.2, 115.1, 114.8, 112.4, 106.6, 55.6, 30.1, 21.6, 20.6. HRMS (ESI-TOF): calcd. for $C_{27}H_{24}NO_3$ $[M + H]^+$ 410.1751; found 410.1753.

Synthesis of Compound 4

Compound 1 (150 mg, 0.5 mmol), **Compound 3** (205 mg, 0.5 mmol), and $Zn(OAc)_2$ (240 mg, 1.3 mmol) were dissolved in ethanol (8 mL), followed by the addition of piperidine (148 µL, 1.5 mmol). The reaction mixture is stirred at 80 °C for 7 h in a sealed tube. The reaction mixture was then cooled to room temperature and cold diethyl ether (30 mL) was added to facilitate the precipitation, then collected by filtration. The crude product was purified by flash column chromatography eluting with (DCM/MeOH, 20:1, v/v) to afford **compound 4** as a blue solid (292 mg, 85% yield). ^{1}H NMR (400 MHz, $CDCl_3$) δ 9.53 (d, J = 6.8 Hz, 1H), 8.43 (d, J = 8.0 Hz, 1H), 8.29 (d, J = 14.8 Hz, 1H), 8.07 (d, J = 8.4 Hz, 1H), 8.03 – 7.97 (m, 1H), 7.87 (d, J = 6.8 Hz, 1H), 7.80 – 7.72 (m, 1H), 7.38 – 7.29 (m, 2H), 7.18 – 7.10 (m, 5H), 7.04 (d, J = 15.2 Hz, 1H), 6.99 (d, J = 8.4 Hz, 1H), 6.96 – 6.89 (m, 2H), 6.82 (d, J = 1.6 Hz, 1H), 6.71 (dd, J = 8.4, 2.0 Hz, 1H), 6.69 (s, 1H), 5.09 (q, J = 7.2 Hz, 2H), 3.86 (s, 3H), 2.67 (t, J = 6.0 Hz, 2H), 2.62 (t, J = 6.0 Hz, 2H), 1.94 – 1.82 (m, 2H), 1.69 (t, J = 7.2 Hz, 3H). ^{13}C NMR (100 MHz, DMSO-d_6) δ 156.6, 154.2, 153.3, 152.1, 149.6, 146.5, 145.2, 138.9, 137.5, 137.4, 134.3, 129.6, 128.2, 127.8, 127.4, 126.9, 126.5, 126.1, 125.7, 124.2, 123.7, 118.5, 116.4, 115.3, 115.2, 114.3, 113.8, 112.3, 106.0, 55.3, 51.0, 28.8, 24.4, 20.3, 14.9. HRMS (ESI-TOF): calcd. for $C_{39}H_{35}N_2O_2$ $[M + H]^+$ 563.2693; found 563.2687.

Synthesis of POH

To a solution of **compound 4** (60 mg, 0.145 mmol) in dry CH_2Cl_2 (1 mL) was added BBr_3 (3 mL, 2 M in CH_2Cl_2) at 0 °C. The reaction mixture was stirred at 0 °C for another 3 h. Then, the reaction was quenched with a saturated solution of $NaHCO_3$ (5 mL) at 0 °C and extracted with a mixture of CH_2Cl_2/MeOH (3 ✂ 10 mL, 10:1, v/v). The combined organic phase was dried over anhydrous $MgSO_4$, filtered, concentrated in vacuo, and the residue was purified by flash column chromatography eluting with (DCM/MeOH, 20:1, v/v) to afford **POH** as a blue solid (36 mg, 62% yield). ^{1}H NMR (400 MHz, DMSO-d_6) δ 9.63 (s, 1H), 8.98 (d, J = 6.8 Hz, 1H), 8.81 (d, J = 8.0 Hz, 1H), 8.38 (d, J = 15.2 Hz, 1H), 8.36 (d, J = 8.8 Hz, 1H), 8.29 (d, J = 6.8

Hz, 1H), 8.16 – 8.09 (m, 1H), 7.87 (t, J = 8.0 Hz, 1H), 7.35 (t, J = 8.0 Hz, 2H), 7.31 (d, J = 14.0 Hz, 1H), 7.17 (d, J = 8.4 Hz, 1H), 7.13 – 7.06 (m, 3H), 7.04 – 6.97 (m, 2H), 6.88 (s, 1H), 6.87 – 6.78 (m, 3H), 6.56 (dd, J = 8.4, 2.0 Hz, 1H), 4.85 (q, J = 7.2 Hz, 2H), 2.70 (t, J = 6.0 Hz, 2H), 2.63 (t, J = 5.6 Hz, 2H), 1.85 – 1.74 (m, 2H), 1.52 (t, J = 7.2 Hz, 3H). ^{13}C NMR (100 MHz, DMSO-d_6) δ 155.7, 154.8, 153.9, 152.7, 150.4, 147.1, 145.9, 138.1, 138.0, 137.7, 134.9, 130.1, 128.8, 127.9, 127.2, 127.1, 126.7, 126.3, 124.7, 124.1, 119.1, 117.1, 116.6, 115.5, 114.9, 114.4, 112.8, 106.1, 51.5, 29.4, 24.9, 20.9, 15.5. HRMS (ESI-TOF): calcd. for $C_{38}H_{33}N_2O_2$ $[M + H]^+$ 549.2537; found 549.2539.

Characterization data for Compound 1

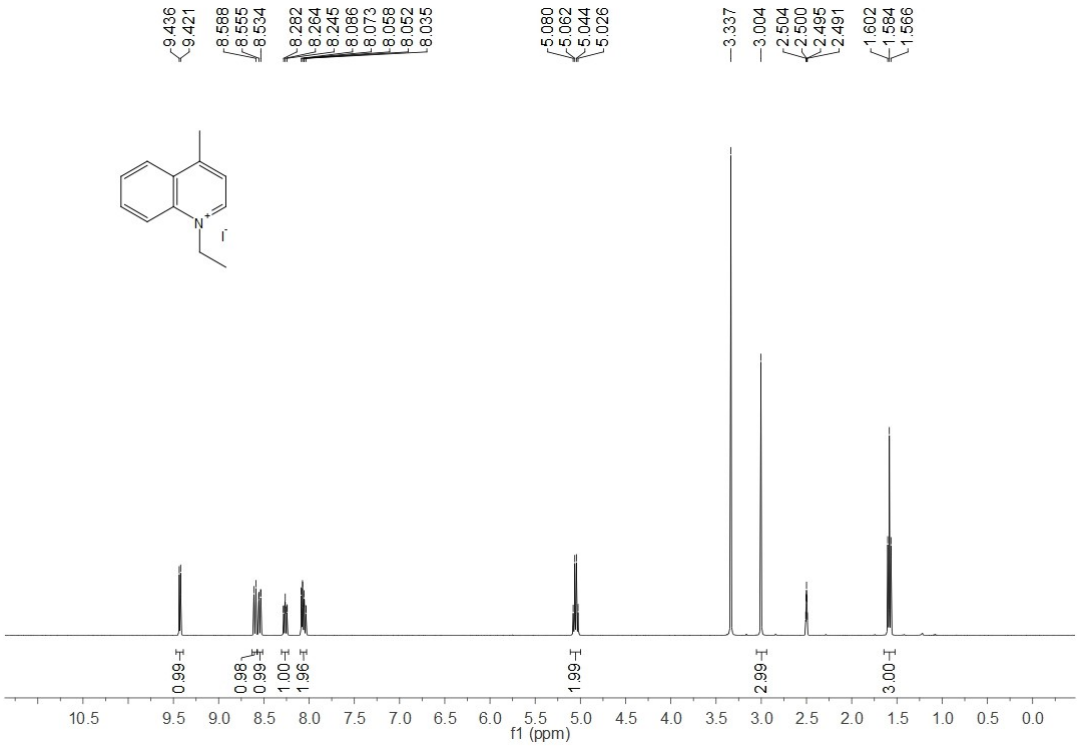

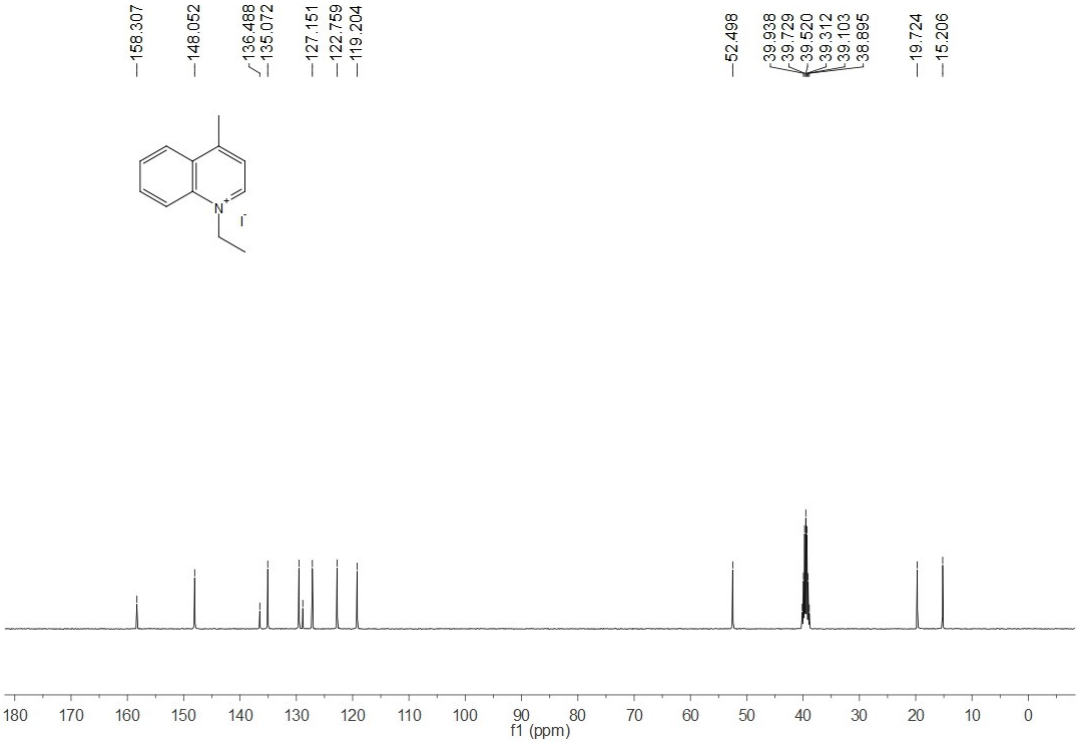

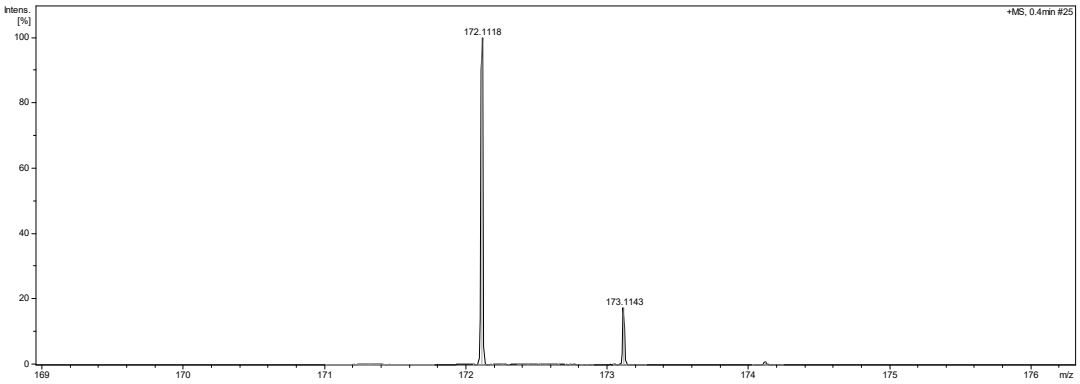
Intens.
[%]
+MS, 0.4min #25
172.1118
173.1143
100
80
60
40
20
0
169
170
171
172
173
174
175
176
m/z

Characterization data for Compound 2

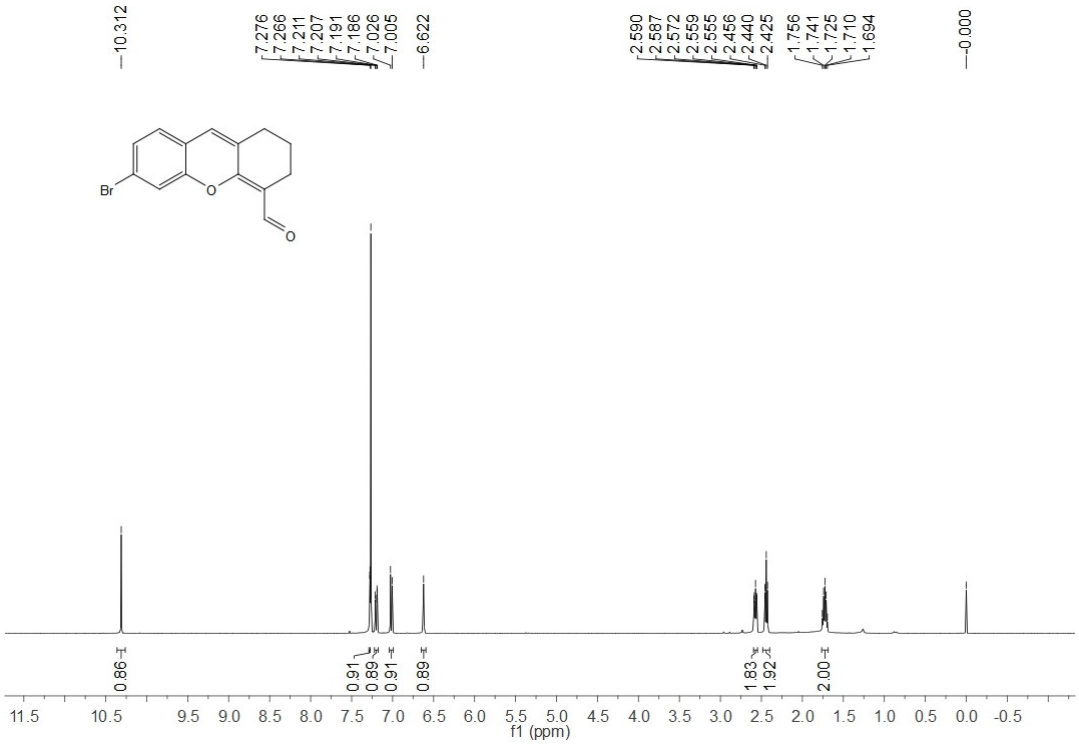

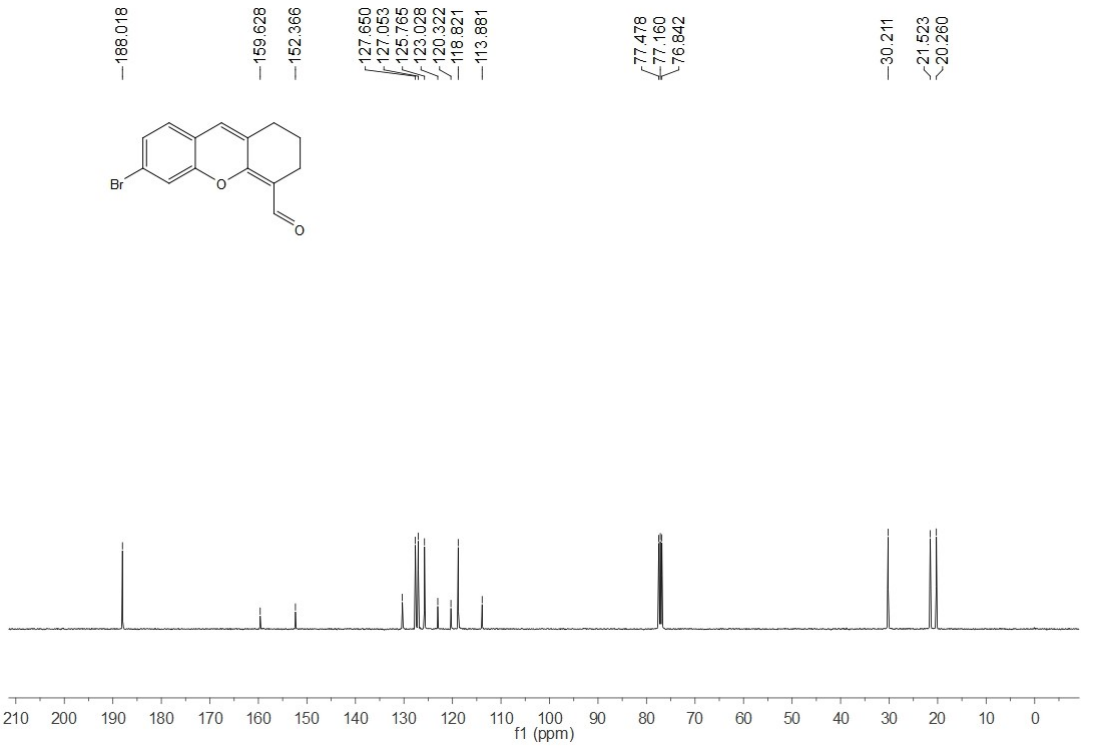
188.018
159.628
152.366
127.650
127.053
125.765
123.028
120.322
118.821
113.881
77.478
77.160
76.842
30.211
21.523
20.260
Br
O
O
210 200 190 180 170 160 150 140 130 120 110 100 90 80 70 60 50 40 30 20 10 0
f1 (ppm)

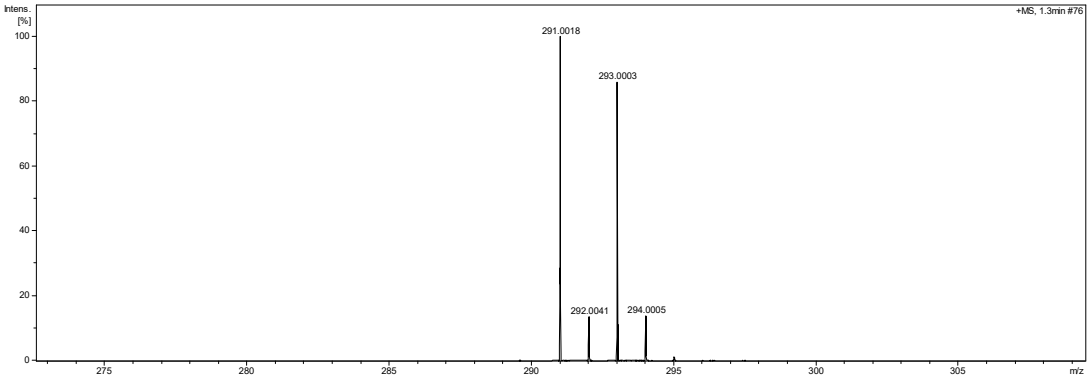
Intens.
[%]
+MS, 1.3min #76
291.0018
293.0003
292.0041
294.0005
100
80
60
40
20
0
275
280
285
290
295
300
305
m/z

Characterization data for Compound 3

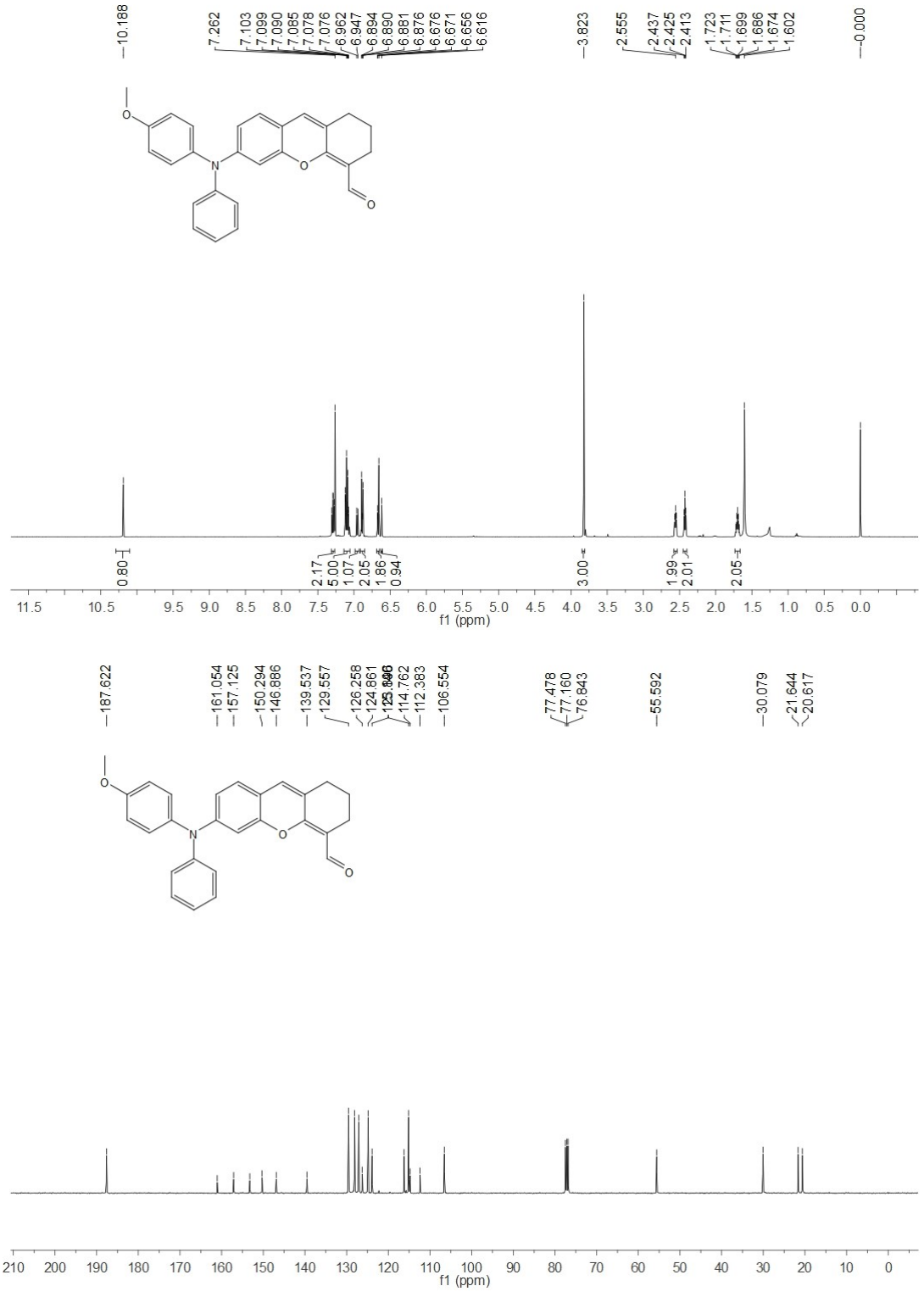

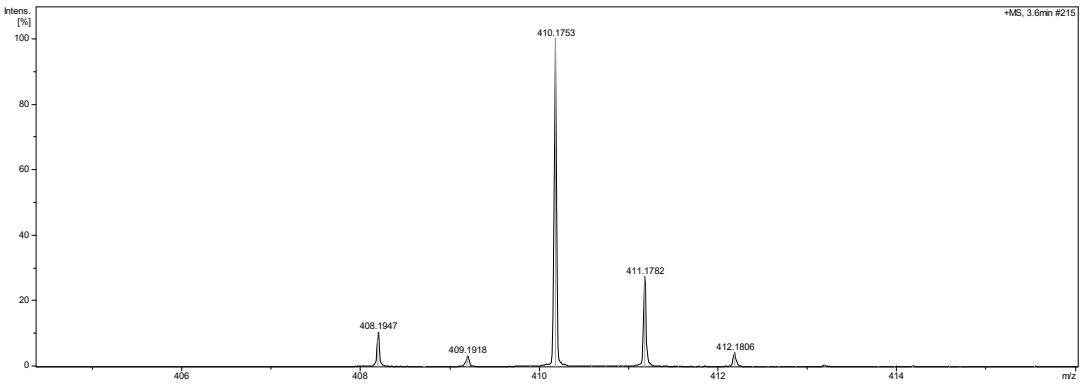
Intens.
[%]
+MS, 3.6min #215
100
80
60
40
20
0
410.1753
411.1782
408.1947
409.1918
412.1806
406
408
410
412
414
m/z

Characterization data for Compound 4

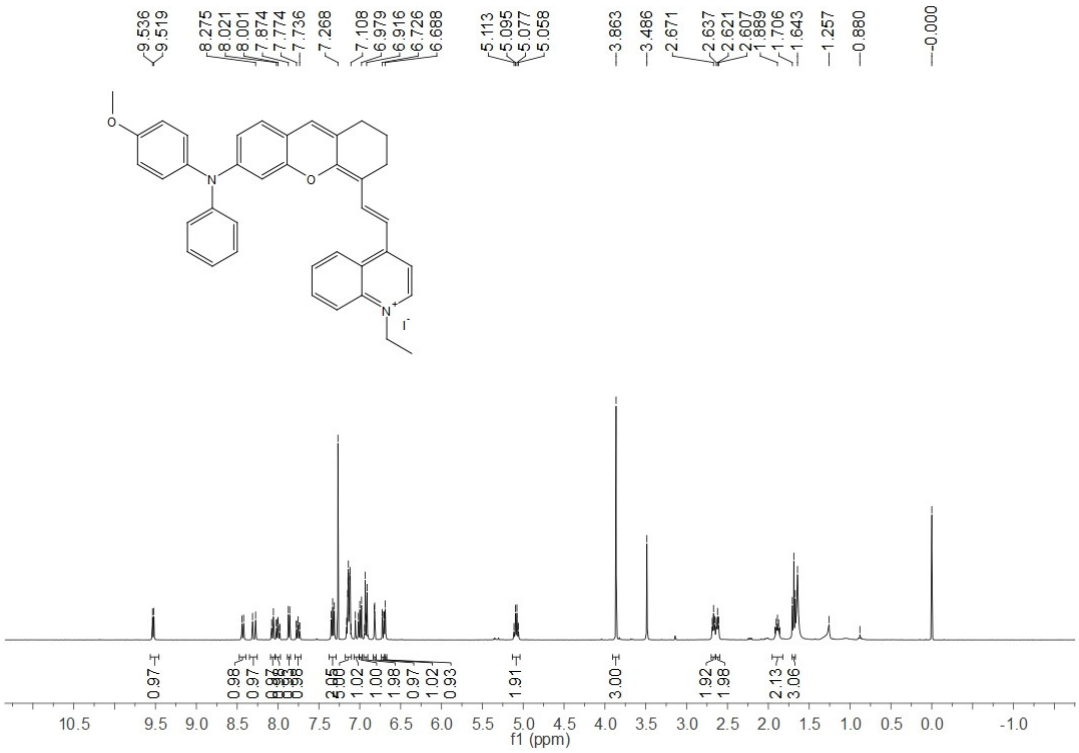

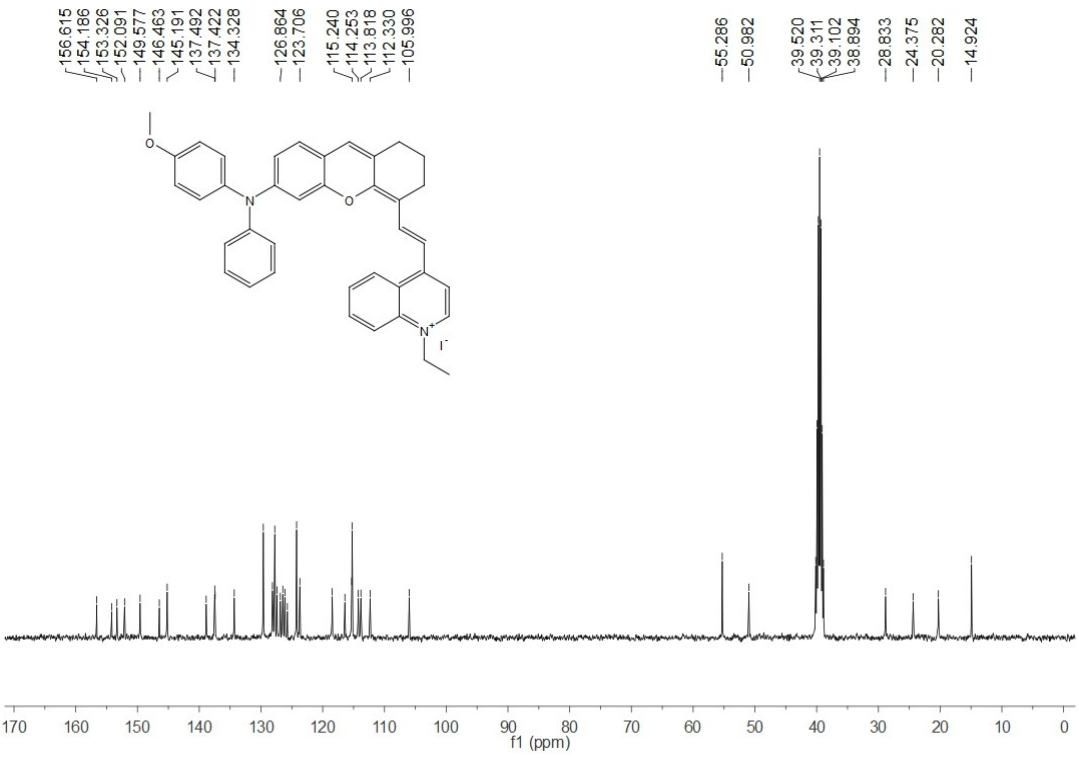

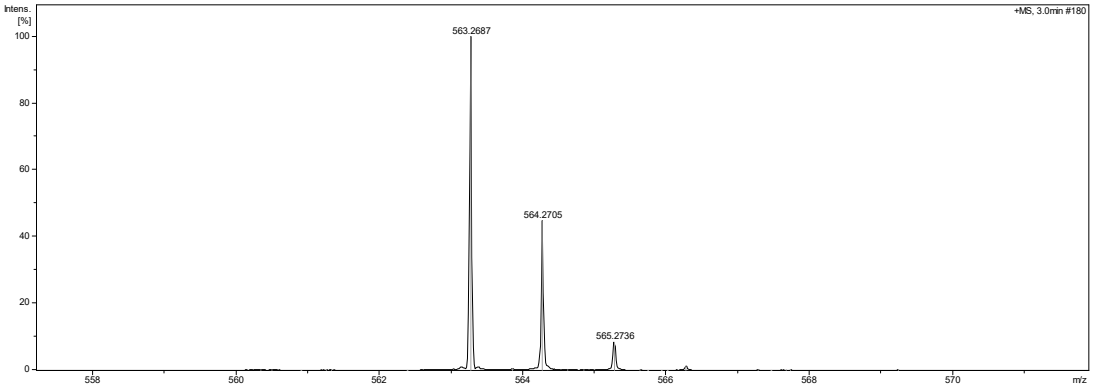
Intens.
[%]
+MS, 3.0min #180
563.2687
564.2705
565.2736
100
80
60
40
20
0
558
560
562
564
566
568
570
m/z

Characterization data for POH

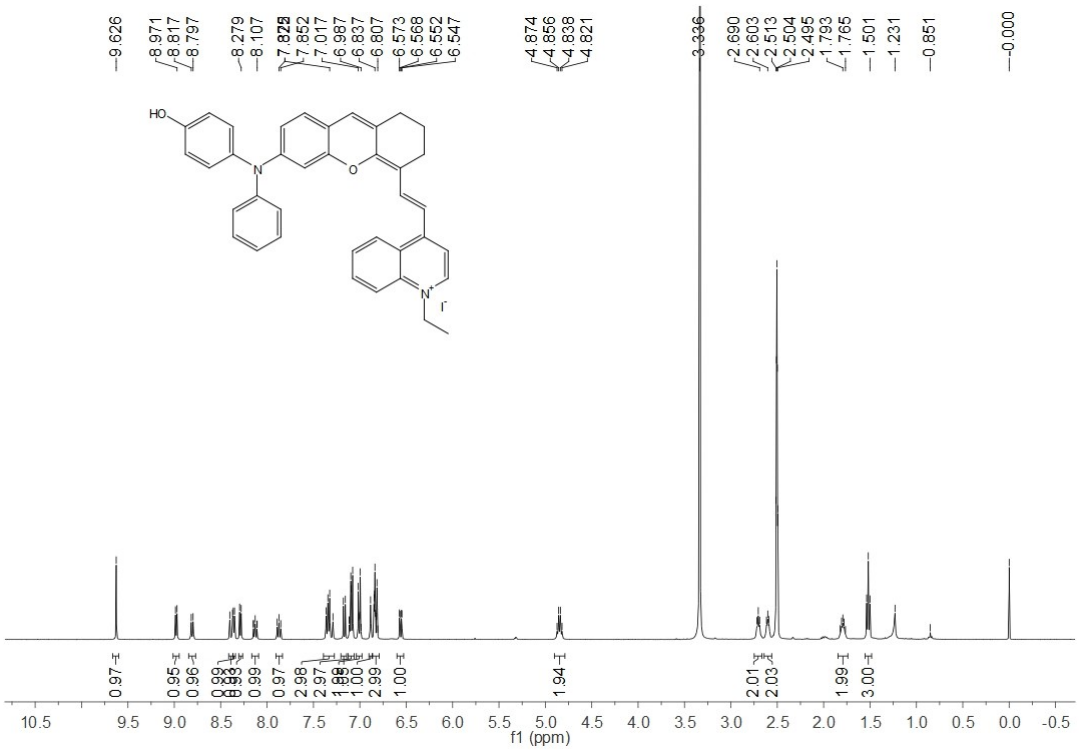

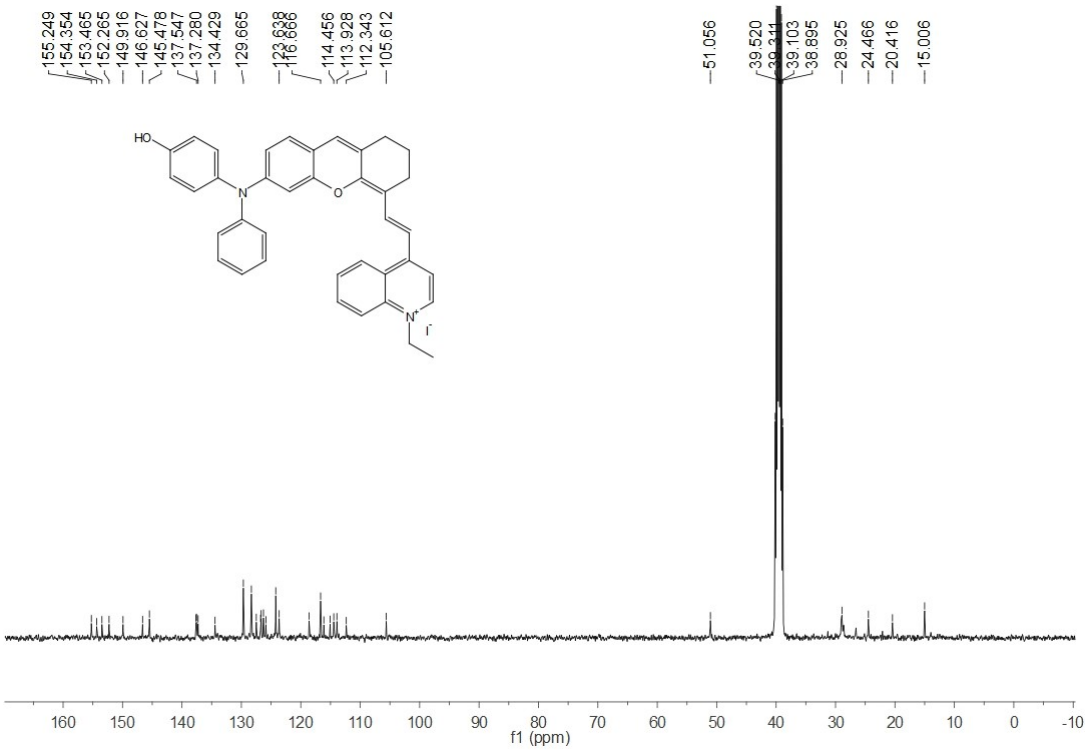

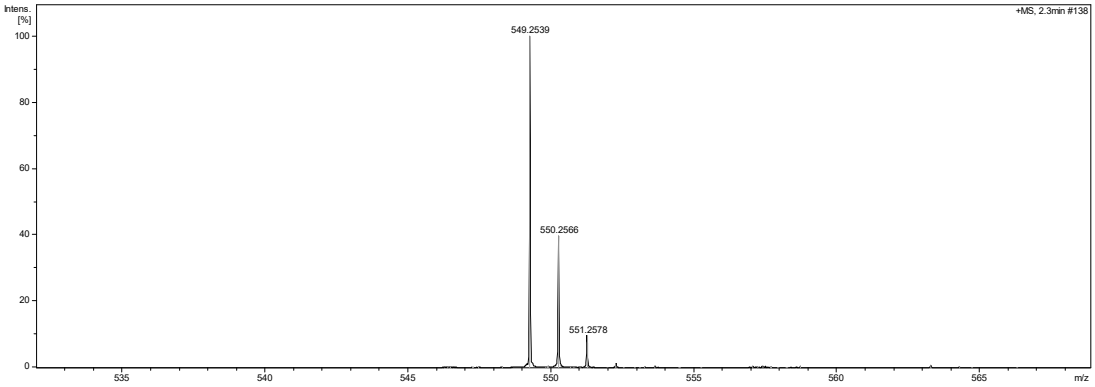
Intens.
[%]
+MS, 2.3min #138
549.2539
550.2566
551.2578
100
80
60
40
20
0
535
540
545
550
555
560
565
m/z

Supplementary figures

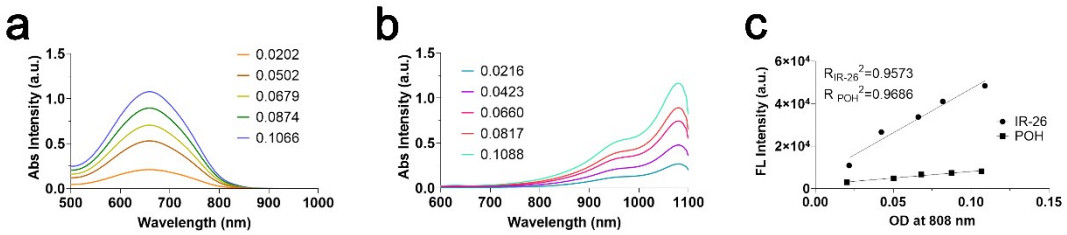

Figure S1. Optical absorbance spectra of a series of five solutions of a) POH in PBS and b) IR-26 in DCE with absorbance values at 808 nm were in the range from ~0.02 to ~0.1. c) The integrated NIR-II signal intensities (900−1500 nm) of the above samples plotted against the absorbance at 808 nm for POH in PBS, respectively.

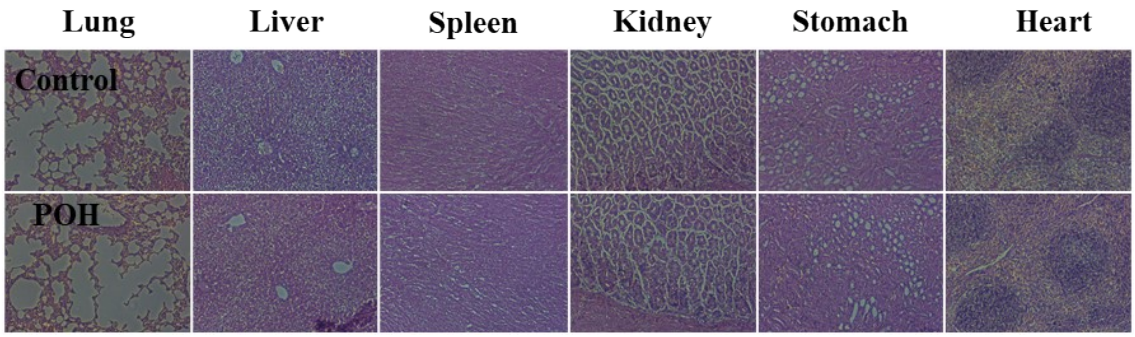

Figure S2. Histological evaluation of main organs after intravenous administration of POH.

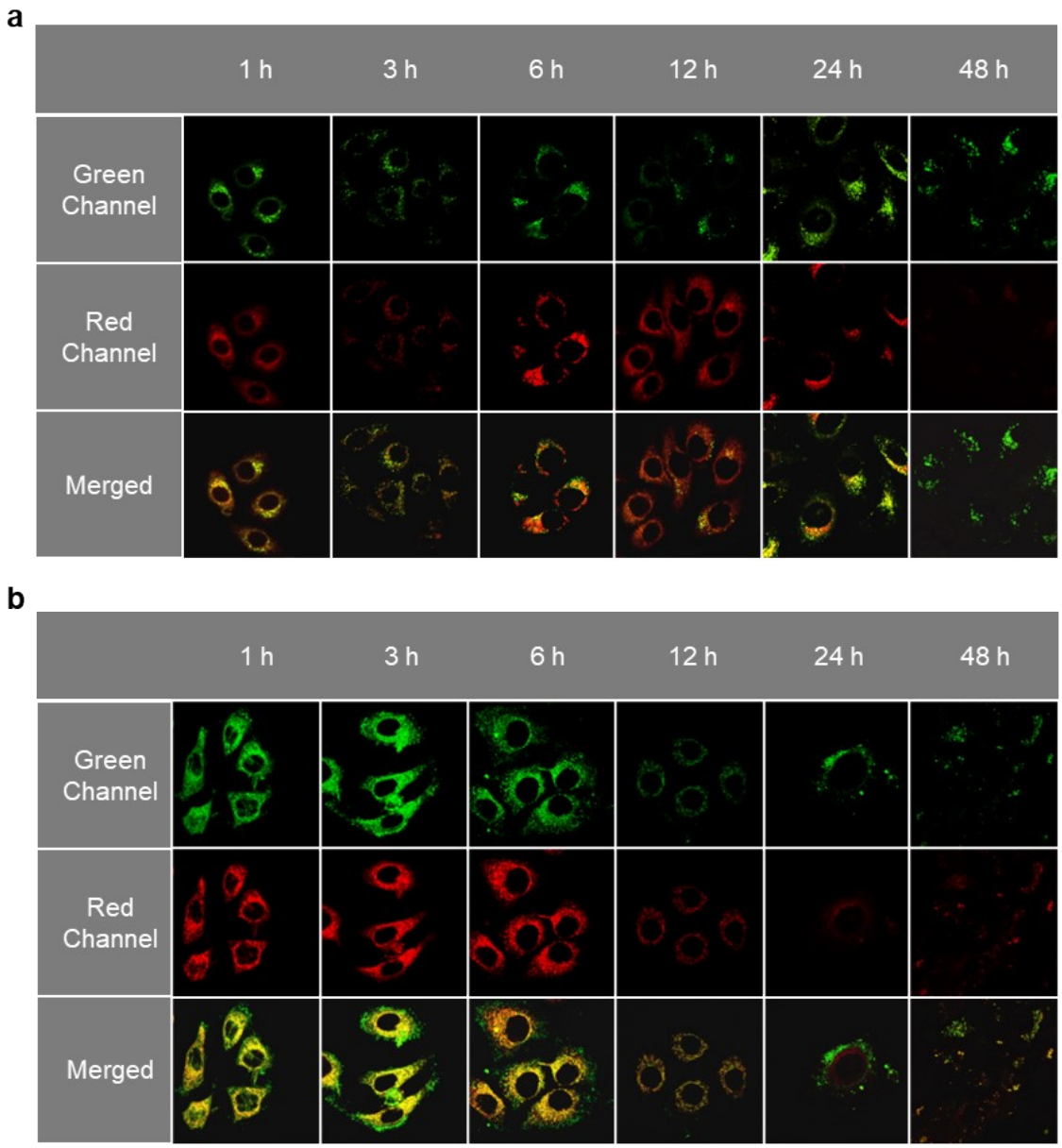

Figure S3. The subcellular recombination degree of POH in HeLa cells changed with time.

Colocalization images of HeLa cells co-incubated with POH for the red channel (10 μM, Ex =

640 nm, collected from 680−800 nm) and the corresponding organelle targeting dyes for the green channel for a) lysosome and b) mitochondria (LysoTracker Green, 100 nM, Ex = 488 nm, collected from 490−550 nm; MitoTracker Green, 100 nM, Ex = 488 nm, collected from 490−550 nm).

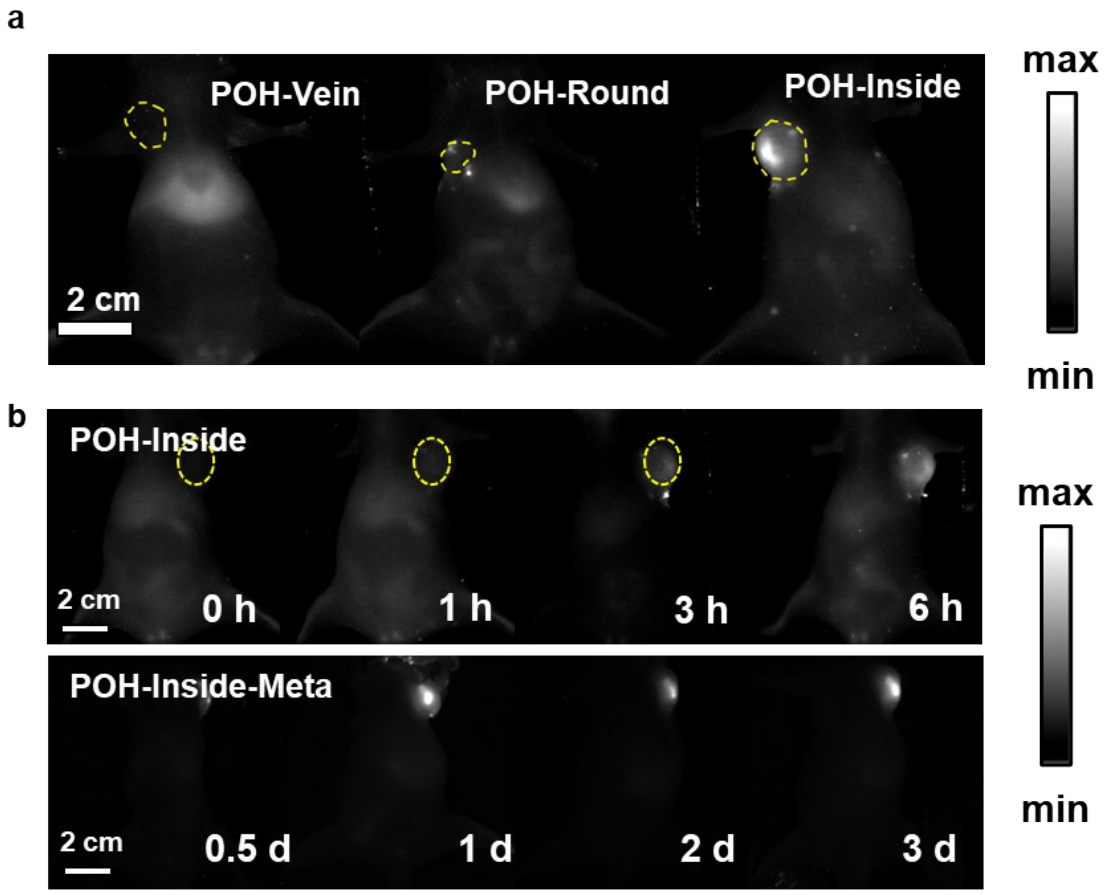

Figure S4. Different imaging effects of POH on tumor tissue. a) Effect of NIR imaging on tumor *in vivo* under different dosing modes (injection dosage, 100 μM, 25 μL; imaging condition: 808 nm laser excitation with 65 mW/cm^2 power density, 900 + 1000 nm long-pass filters). b) Changes of tumor near-infrared signal over time after intratumoral injection.

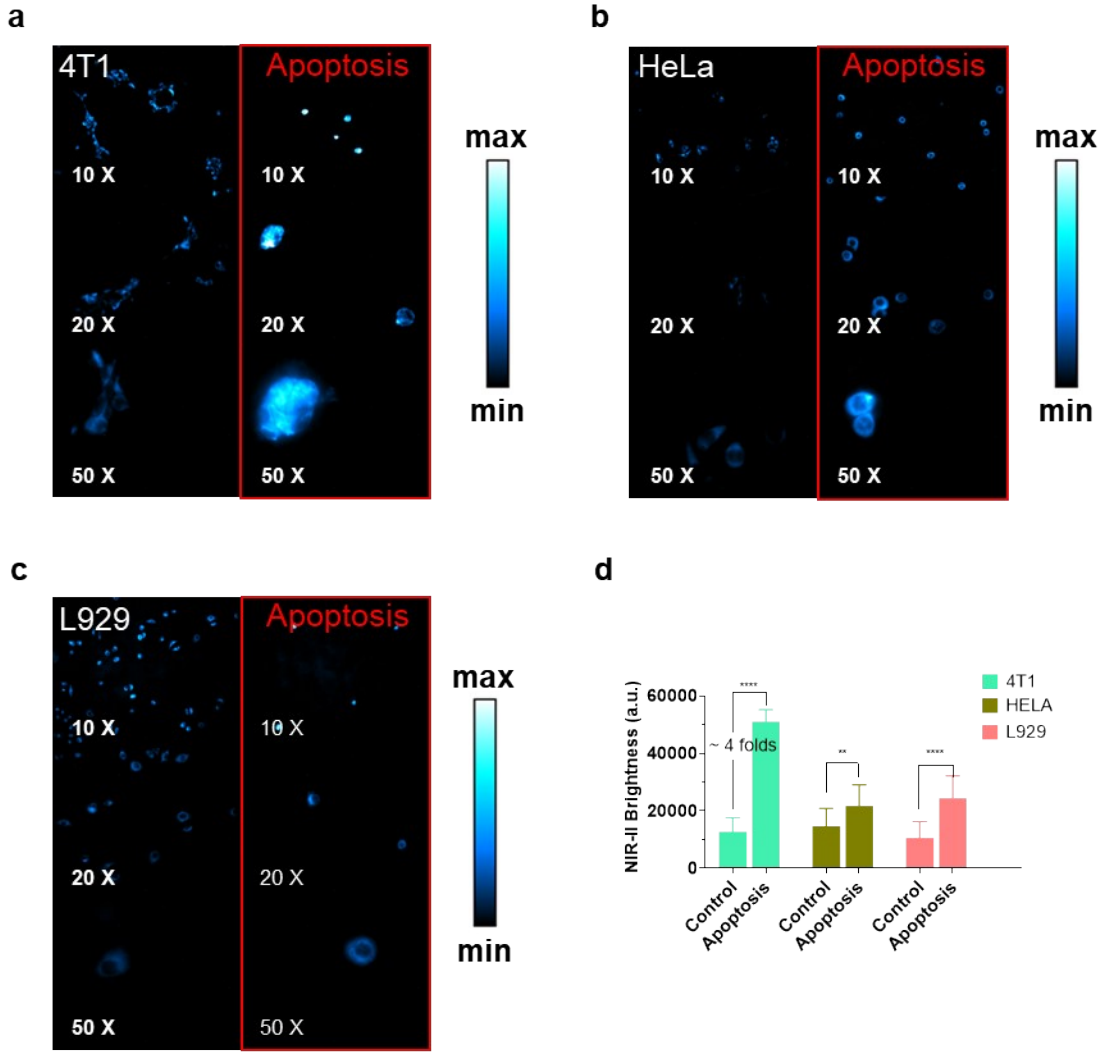

Figure S5. Fluorescent images of apoptotic cells and control cells. a-c) Fluorescence images of three different cells (4T1, HeLa, L929) at different magnifications under NIR microscopy, and d) statistical values of fluorescence signals. All data are expressed as mean ± SD. Significance was defined as * $p < 0.05$, ** $p < 0.01$, *** $p < 0.001$, **** $p < 0.0001$.

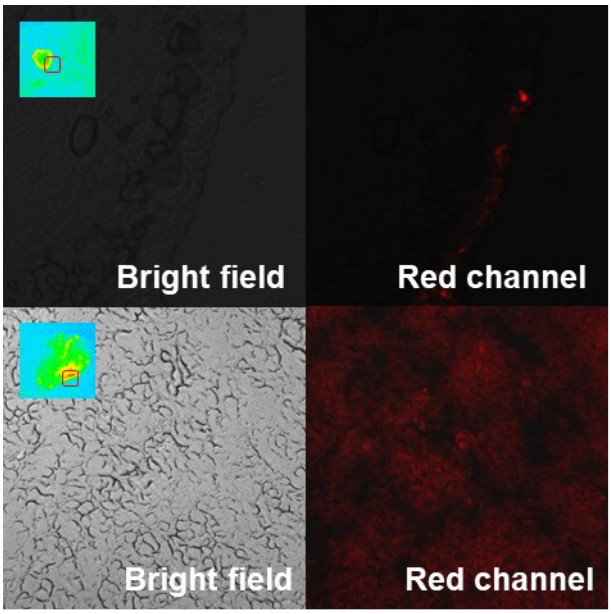

Figure S6. Fluorescence images at the subcellular level of frozen sections of tumor tissue showing responsive signals.

4. Author Contributions

In this work, Han Tianyang was responsible for writing the article, optical data characterization, data processing, and animal experiments. Lin Lihao and Jiang Huizhong conducted animal and cell experiments in this study. Zhang Yuewei was dominated in the structural design and organic synthesis of molecular probes and also contributed to the writing and revision of the article. Fan Li participated in the writing and revision of the article in this study.

5. Conflicts of interest

The authors declare no conflicts of interest.

6. Acknowledgement

This work was supported by the Joint Laboratory of Opto-Functional Theranostics in Medicine and Chemistry, the First Hospital of Jilin University. All animal experiments were conducted under institutional guidelines and were approved by the Experimental Animal Ethical Committee of the First Hospital of Jilin University (Protocol number: 20210642). We express our gratitude for the financial assistance received from the Program of Science and Technology Development Plan of Jilin Province (YDZJ202201ZYTS618, YDZJ202301ZYTS312), Outstanding Youth Training Program of Jilin City (20230103015), National Natural Science Foundation of China (81901814).

7. Reference

[1] Q. Yang, Z. Hu, S. Zhu, R. Ma, H. Ma, Z. Ma, H. Wan, T. Zhu, Z. Jiang, W. Liu, L. Jiao, H. Sun, Y. Liang, H. Dai, *J. Am. Chem. Soc.* **2018**, *140*, 1715-1724.